Electronic Supplementary Material (ESI) for ChemComm.

Electronic Supplementary Information (ESI)

Rapid and Directly Interpretable Antimicrobial Susceptibility Profiling by Continuous Microvolume-Electroanalysis of Ferricyanide-Mediated Bacterial Respiration

Krittamate Buppasirakul, Wipa Suginta, and Albert Schulte*

School of Biomolecular Science and Engineering

Vidyasirimedhi Institute of Science and Technology (VISTEC)

Wang Chan Valley, Rayong 21210, Thailand

* Corresponding author, email: albert.s@vistec.ac.th

Experimental Section

1. Materials

Potassium ferricyanide was purchased from Thermo Fisher Scientific, USA; Potessium ferrocyanide trihydrate from Sigma-Aldrich, USA; ammonium formate from Acros Organics, Belgium; D-glucose from Carlo Erba, Italy; Luria-Bertani (LB) broth containing 10 g/l tryptone, 5 g/l yeast extract and 10 g/l NaCl from Angel Yeast, China; ampicillin sodium from Formedium, England; kanamycin sulfate from Bio Basic, Canada; nalidixic acid from Glentham Life Science, England; doxycycline hyclate, imipenem monohydrate, ciprofloxacin and cefepime dihydrochloride monohydrate from Chem-Impex International, England; and *E. coli* DH5α cells were purchased from Invitrogen, USA.

2. Bacterium cultivation and colony counting

A Gram-negative E. coli DH5α was chosen as the model organism due to its routine use in the laboratory and ease of handling. Typically, bacterial stocks were stored in 50% glycerol in LB broth at -80°C. For cultivation, the frozen stock was thawed and streaked on LB agar plates, followed by incubation at 37°C for 16 hours. The resulting bacterial colonies were then picked and cultivated aerobically in LB broth supplemented with 2 g/l glucose at 37°C for 16 hours with shaking at 180 rpm. Colony counting was afterward performed on the resulting inoculum by 10-fold serial dilution in 0.9% NaCl, spreading 100 µl aliquot on agar plates, allowing them to grow at 37°C for 16 hours, and then counting visible colonies on plates with less than 300 colonies. Bacterial density in colony forming units per ml (CFU/ml) was averaged from triplicate counting and calibrated with optical density at 600 nm (OD_{600})

3. Antibiotic stock preparation

Seven model antibiotics were chosen from different classes; they were kanamycin from the aminoglycosides, doxycycline from the tetracyclines, ampicillin from the penicillins, imipenem from the carbapenems, cefepime from the cephalosporins and ciprofloxacin and nalidixic acid from the fluoroquinolones. Stock solutions of the antibiotics were prepared by dissolving antibiotic powders in appropriate solvents. Kanamycin, doxycycline, ampicillin, imipenem and cefepime were dissolved in deionized water to a concentration of 1,600 µg/ml for cefepime, and 5,120 µg/ml for all the others. Ciprofloxacin was first dissolved in 0.1 M HCl at 20% v/v before being diluted with deionized water to the final concentration of 1,600 µg/ml. Nalidixic acid was first dissolved in 1.0 M NaOH at 5% v/v before being diluted with deionized water to the final concentration of 5,120 µg/ml. The resulting stock solutions were sterilized with a 0.2-µm filtration membrane and stored at -20°C until use.

4. Antibiotic treatment and ferricyanide incubation assay

The procedure here was adapted from our group's previous study (Chotinantakul et al.[1]). Antibiotic solutions were prepared as 2-fold serial dilutions in 500 µl of LB broth, ranging from 256 to 0.125 µg/ml for ampicillin, kanamycin, doxycycline, imipenem, and nalidixic acid, and from 8 to 0.004 µg/ml for ciprofloxacin and cefepime. Overnight bacterial cultures were diluted into the antibiotic solutions to achieve a final density of 1 x 10^6 CFU/ml after keeping them on ice for 15 minutes. A positive control without antibiotics was prepared similarly. The cell-antibiotic solutions were incubated in a thermomixer at 37°C for 3 hours with shaking at 800 rpm. After incubation, cultures were centrifuged at 8,000 g for 10 minutes to remove the antibiotics. Cell pellets were washed with PBS and centrifuged again using the same parameters. The cell pellets were then resuspended in 500 µl of a solution containing 40 mM potassium ferricyanide and 20 mM ammonium formate as a respiration substrate in LB broth. The resuspended samples were incubated in the thermomixer at 37°C for 1 hour with shaking at 800 rpm. A blank solution of ferricyanide without cells served as a control. Lastly, the resulting suspensions were centrifuged again to extract ferri/ferrocyanide supernatant for further electrochemical measurement.

5. Electrochemical apparatus and pre-measurement process

The potentiostat used in all electrochemical experiments was a Gamry Reference 600+, Gamry Instruments, USA. The working electrode was a 3-mm Pt disk, also from Gamry Instrument. The Pt vessel of the miniaturized electrochemical cell was rolled from a thin high-purity Pt foil from Goodfellow, England.

Prior to the measurement, the rolled Pt foil was cleaned by flaming, and the Pt working electrode was polished using alumina slurry with particle sizes of, first, 1.0 µm and, second, 0.4 µm. Subsequently, the Pt foil was placed on the insulator jacket of the invert-upright working electrode by centering the Pt disk of the working electrode to the hollow of the Pt foil, avoiding electrical contact. This enclosed the bottom of the Pt cylinder to fabricate the mini-cell with the Pt vessel as the counter- electrode. The potentiostat was connected to the working and counter electrode in a two-electrode configuration. Prior to the measurement, the electrodes were pre-conditioned by applying the step pulses to the blank control for 10 cycles.

6. Investigation of the ferricyanide electroanalysis performance of the two-electrode mini-cell and its capability for ecAST testing.

Cyclic voltammetry was conducted with a scan speed of 100 mV/s in a mixed solution of 20 mM ferricyanide and 20 mM ferrocyanide in 0.1 M KCl in the mini-cell that was either used as the proposed two-electrode or as standard three-electrode with the commercial Ag/AgCl reference electrode. The relationship between the magnitude of the anodic and cathodic cyclic voltammogram (CV) peak currents and the scan rate were inspected in the two-electrode cell for trials that used at 10, 50, 100, 250, 500, and 1000 mV/s as scan speed. With the acquired data was converted into plots of the anodic and cathodic peak currents against the square root of scan rate.

The suitability of the mini-cell in ferricyanide-mediated ecAST was investigated using artificial samples with various ratios of ferrocyanide/ferricyanide, which were adjusted to values that imitated different degrees of bacterial conversion of ferricyanide in the cell grow/respiration step of the assay. CVs for the sample set were carried out with scans from -0.4 to 0.4 V to observe for the given Fe(III)/Fe(II) ratios the related ferrocyanide oxidation peaks and use the information to identify the appropriate oxidation potential for the amperometric measurements of the ecAST testing. Later, chronoamperometry with a 180 s recording time was conducted on a range of imitating test samples to confirm the suitability of the selected oxidation potential in detecting the ferrocyanide, which ultimately was the indicator of surviving bacterial cell respiration.

7. Broth microdilution: a conventional antimicrobial susceptibility testing (AST)

The microdilution was conducted following the standardized protocol by the Clinical & Laboratory Standards Institute (CLSI), except the media was replaced with the LB broth.[2] Briefly, wells of 96-well plates were filled with 100 μl of antibiotic serial dilutions, the same as those in the electrochemical experiment. The bacterial inoculum was diluted into the antibiotic panel to yield a final density of 5 x 10^5 CFU/ml. The positive control was made of cell suspension in LB broth without antibiotics, and the negative control was 10% DMSO in the LB broth. Three biological replicates were made for each antibiotic. The prepared microdilution panels were incubated at 37°C for 16 hours. Subsequently, bacterial growth and susceptibility of the incubated panels were measured spectrophotometrically to obtain OD_{600}. The measured OD_{600} was converted to % Viability to assess the quantitative proportion of the bacterial growth in the testing antibiotics and further used for validating the % Viability obtained by the proposed electrochemical measurement. The equation for calculating % Viability is like that used for the electrochemical result but with the measured OD_{600} used instead of the peak currents. The equation is:

$$\%\ \text{Viability} = \frac{\left(A_{+\text{drug}} - A_0\right)}{\left(A_{-\text{drug}} - A_0\right)} \times 100\ \%$$

where A_{+drug} is the measuring OD_{600} from the sample exposed to an antibiotic, A_{-drug} is that of the positive control, and A_0 is that of the negative control.

Discussion section

1. Electroanalyses performance of the two-electrode mini-cell

We evaluated the performance of our custom two-electrode mini-cell, featuring a 3-mm Pt disk as the WE and a Pt mini-vessel as the combined CE/RE, through fundamental electrochemistry experiments. Initially, we examined the potential shift of the redox peaks in the CVs of the two-electrode system relative to the location of the CV current peaks of the three-electrode version, which was equipped with an Ag/AgCl RE. This comparison was conducted for a mixed solution of 20 mM ferricyanide (Fe(III)) and 20 mM ferrocyanide (Fe(II)) in 100 mM KCl at a scan rate of 100 mV/s (Fig. S1A). Clearly revealed was a significant negative potential shift for the ferricyanide/ferrocyanide redox in the two-electrode cell, approximately

460 mV for the anodic peak and 480 mV for the cathodic peak, compared to the three-electrode configuration. Despite this shift, the two-electrode cell generated a CV pattern that was well consistent with the typical duck shape observed in the three-electrode system. Subsequently, we explored the correlation between the CV peak currents and the scan rate across a range from 10 mV/s to 1000 mV/s. Figure S1B(I) is an illustration of the increasing peak currents in the CVs with the scan rate rise. To verify appropriate electrode/electrochemical cell characteristics, the anodic and cathodic peak currents were plotted against the square root of the scan rate, according to the Randles-Sevcik equation. Fig. S1B(II) displays the resulting linear relationships for both anodic and cathodic peaks within the tested scan rate range, suggesting a diffusion-controlled and quasi-reversible behavior of the redox analyte in our miniaturized two-electrode cell.[3] The observed agreement with theory confirmed the practicality of the system for fundamental electroanalysis despite the absence of an actual RE.

2. Feasibility of the fabricated mini-cell in ferricyanide-mediated electrochemical AST

To investigate the capabilities of the two-electrode cell in electrochemical AST (ecAST), electroanalysis trials were conducted on samples that were artificially prepared to mimic varying extents of bacterial conversion of Fe(III) to Fe(II). In our experiments, the incubation of bacterial cells with Fe(III) results in the reduction of Fe(III) to Fe(II) via bacterial respiration. The growth control, without antibiotic exposure, leads to a high extent of Fe(III) conversion, as the bacterial metabolism is functional in a healthy state, whereas samples of bacteria exposed to effective antibiotics are expected to exhibit lower metabolic conversion corresponding to the concentration of the antibiotics. Therefore, the imitating samples were prepared as mixtures with various ratios of Fe(III) and Fe(II) in LB broth according to the theoretical conversion percentage (% conversion). The starting concentration of Fe(III) was, for instance, in our work 40 mM, and 40 mM in a 'respiration' sample thus referred to a 0 % conversion. A 'respiration' sample with a 5 % conversion rate referred on the other hand to 38 mM Fe(III) and 2 mM Fe(II) to mimic a 5 % turnover of Fe(III) to Fe(II).

The positive-scan CVs from -0.4 to 0.3 V of the imitating samples with different % conversions are shown in Fig S2A. Observably, the current and potential of anodic peaks of Fe(II) oxidation around 0.0 to 0.1 V vary according to the concentration of Fe(II); higher ratios of Fe(II)/Fe(III) or higher % conversion result in a positively shifted anodic peak with increasing peak currents. A CV of a growth control was added to this observation to estimate the expected maximum % conversion of our assay. The growth control response aligns with this trend, suggesting that % conversion is slightly less than 25%. According to this trend, we selected 300 mV as a detecting potential for our pulse amperometric experiment to ensure that the potential was sufficiently positive to oxidize Fe(II) in the analyte maximally.

To validate the working oxidation potential and capability of the two-electrode cell in amperometry, chronoamperometry was conducted on the imitating samples with a range of % conversion. Fig S2B(I) displays the resulting amperograms, showing that the amperometric current responses increase with the concentration of Fe(II). The limiting currents at 180 s were extracted from triplicate measurements and plotted against % conversion. As shown in Fig S2B(II), a linearity with an R^2 of 0.9924 was found from 1 to 40 % of Fe(III) conversion. This specifies the capability of the proposed two-electrode cell in amperometric sensing of Fe(II) at 300 mV in samples with varied ratios of Fe(II)/Fe(III) expected to be tested in the ecAST experiments. Taking advantage of the obtained linear regression, the % conversion of the growth controls from our experiment was further estimated. From the average of three independent growth controls, it was found that its % conversion equals about 22.1%, equivalent to about 8.84 mM of Fe(II). Therefore, the

samples in the experiment exposed to effective antibiotics would result in lower concentrations of Fe(II) due to the fact that the bacterial cells are damaged, leading to lower Fe(III) conversion along the established linear trend. This observation further supports the ability and reliability of our two-electrode cell in capturing changes in Fe(II)/Fe(III) concentration dynamics under antibiotic exposure.

3. Comparison of this work to broth microdilution and other redox mediator-based electrochemical ASTs.

Conventional antimicrobial susceptibility tests (AST) are the gold standard for monitoring the effectiveness of antibiotics in inhibiting bacterial growth. Broth microdilution, in particular, relies on the visible turbidity of bacterial growth to establish the minimum inhibitory concentration (MIC), serving as a semi-quantitative breakpoint for susceptibility or resistivity according to standardized criteria. However, conventional methods fall short in delivering interpretable results within a day due to the time-consuming nature of bacterial growth and the duration of antibiotic incubation. In contrast, our method, as one example in the group of ecASTs[4, 5], utilizes ferricyanide as a cell membrane-diffusible indicator of bacterial susceptibility to tested antibiotics. Just 3 hours of antibiotic exposure, followed by an additional 1 hour of ferricyanide reduction through bacterial metabolism, proved sufficient to yield an electrochemically measurable ferrocyanide signal of bacterial viability. Complemented by our proposed continuous pulse amperometry measurement, this allows for the rapid determination of electrochemical minimum inhibitory concentrations (ecMIC). Notably, the determined ecMICs strongly correlate with results from conventional broth microdilution, emphasizing the efficiency and speed of our method in delivering results within a day.

Similarly, other studies employing redox mediator-based electrochemical antimicrobial susceptibility tests (ecASTs) can rapidly and efficiently characterize bacterial susceptibilities. As shown in Table S3, several works utilize resazurin or ferricyanide as metabolic indicators with a variety of sensing platform fabrication and measurement techniques. Despite variations in parameters, antibiotic incubation durations, and measurements, all these studies, like ours, can provide interpretable results within the standard eight working hours. However, our work stands out in that measurements across different samples of antibiotic exposure can be made continuously in a single experiment run, with a very short duration per sample (200 ms). This allows for faster susceptibility observation across all samples compared to other works. Additionally, our sensing platform is simple, reusable, and requires only two electrodes: a reliable commercial macro-WE and an easily rolled thin Pt foil as a concurrent microcontainer and CE/RE without the need for complicated electrode modification, such as casting or functionalization.

Another advantageous feature of ecASTs is their ability to determine MIC faster than conventional methods. Our work validated the MIC of seven antibiotics on E. coli, finding that three of them are equivalent to those determined via the microdilution method, while the rest are still comparable. Several works in Table S3 also interpret MIC and compare its accuracy to conventional methods. It was found that some studies provided accurate MIC values despite shorter or similar antibiotic incubation periods. Compared to our work, however, various factors, such as bacterial strain, population size, antibiotic mode of action, and efficacy within the testing period, contribute to MIC accuracy. Therefore, comparing the accuracy of MIC determination from work to work might be a sophisticated task.

Additionally, it is evident that some works facilitate MIC determination through arrays of electrode wells, where bacterial susceptibilities are quantified simultaneously in wells with different antibiotic concentrations. While this strategy appears promising for quickly quantifying MICs, it may require

complicated (micro)fabrication of electrode arrays and a multichannel potentiostat. In contrast, our two-electrode platform simply requires manual sample switching and the continuous "Pause and Play" operation for rapid MIC semi-quantification at the point of the experiment through raw data interpretation, using a common single-channel, or potentially even a portable or handheld potentiostat. Accordingly, simplicity and low-cost are thus seen as the positive features of the approach of this communication.

Schemes, Figures, and Tables Section

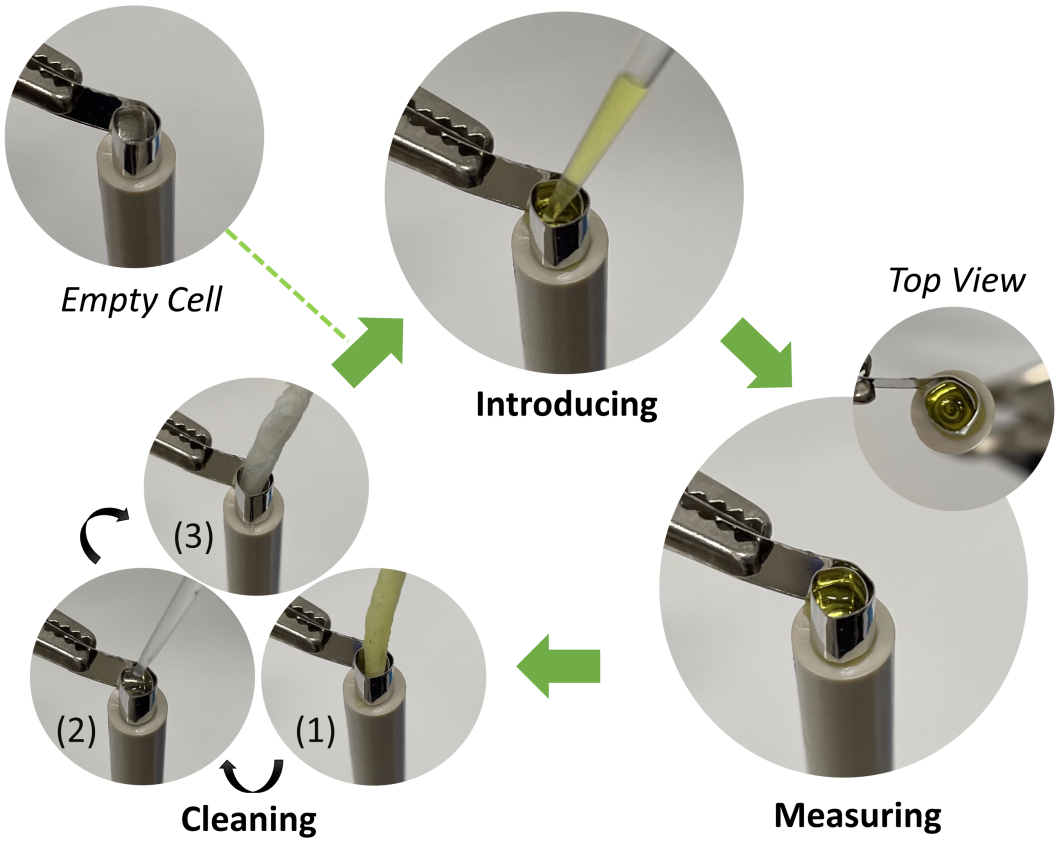

Scheme S1 Photographs that were taken during the operation of a two-electrode mini-cell for an ecAST with the proposed "Pause and Play" procedure. The procedure starts with the cleaned empty cell before introducing the sample of 50 µl. Next is the measuring step, which involves pulse amperometry data acquisition. Then, amperometry is suspended and the mini-cell is cleaned by (1) removing of the tested sample solution using tissue paper, (2) rinsing the cell with DI water, and (3) removing of the DI water using a tissue paper. Lastly, the cell is emptied and readied for the next sample.

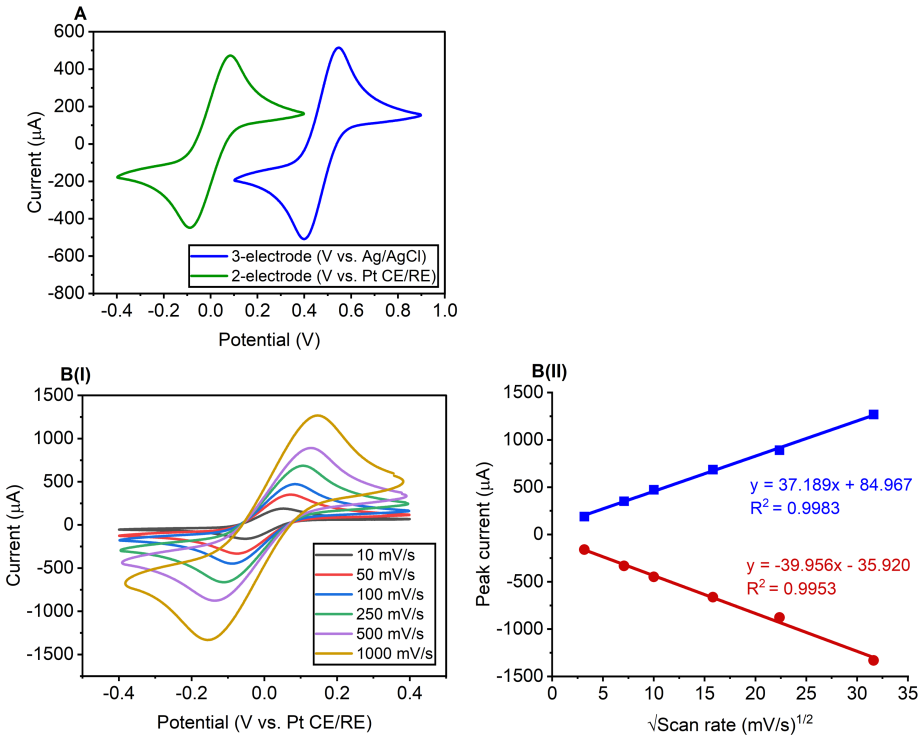

Fig. S1 Electroanalysis in the two-electrode mini-cell. Cyclic voltammetry was performed in the two-electrode mini-cell using a mixed solution of 20 mM ferricyanide (Fe(III)) and 20 mM ferrocyanide (Fe(II)) in 100 mM KCl, revealing a distinctive duck-shaped CV (A, green trace). The position of the CV was shifted to more negative potential compared to the CV of a three-electrode mini-cell that had a proper Ag/AgCl reference electrode (A, blue trace). Further exploration of the relationship between peak currents and scan rates from 10 mV/s to 1000 mV/s for scans from 0.4 V to - 0.4 V demonstrated a concurrent increase (B(I)). Plotting the resulting peak currents against the square root of the scan rate revealed a linear increase for both the anodic peaks (BII, blue) and the cathodic peaks (BII, red).ate revealed a linear increase for both the anodic peaks (upper blue) and the cathodic peaks (lower red).

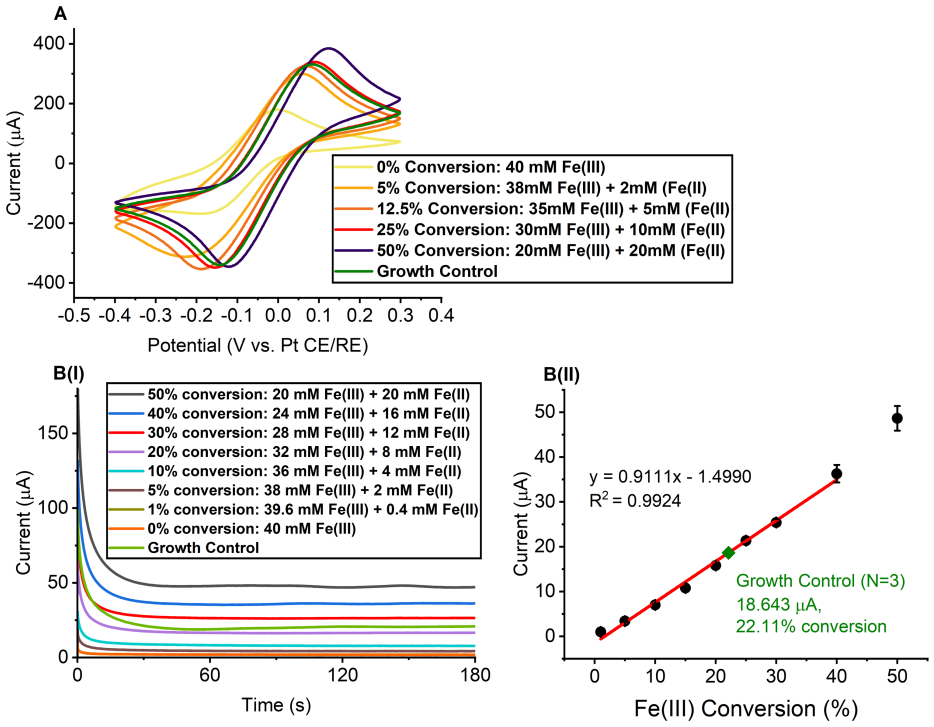

Fig. S2 The Feasibility of the two-electrode mini-cell as arrangement for ferricyanide-mediated ecAST. The study employed samples with varied ratios of Fe(III) and Fe(II) in LB to imitate the conversion percentage (% conversion) of Fe(III) by bacterial respiration. Positive-scanned cyclic voltammograms (CVs) from -0.4 V to 0.3 V of imitating samples with % conversion of 0, 5, 12.5, 25, and 50 % indicate an increasing and shifting anodic peak current of Fe(II) oxidation at 0.0 to 0.1 V following the % conversion and the CV of a growth control aligns with this trend (A). Chronoamperometry of imitating samples with conversions ranging from 0 to 50% at 300 mV shows an increasing limiting current with the concentration of Fe(II) (B(I)). The resulting limiting currents are plotted against % conversion, revealing a linear trend from 1 to 40% conversion (B(II)). The % conversion of the growth control, averaged from three independent experiments, is estimated using the obtained linear trend and found to be 22.11 % (green closed-diamond).

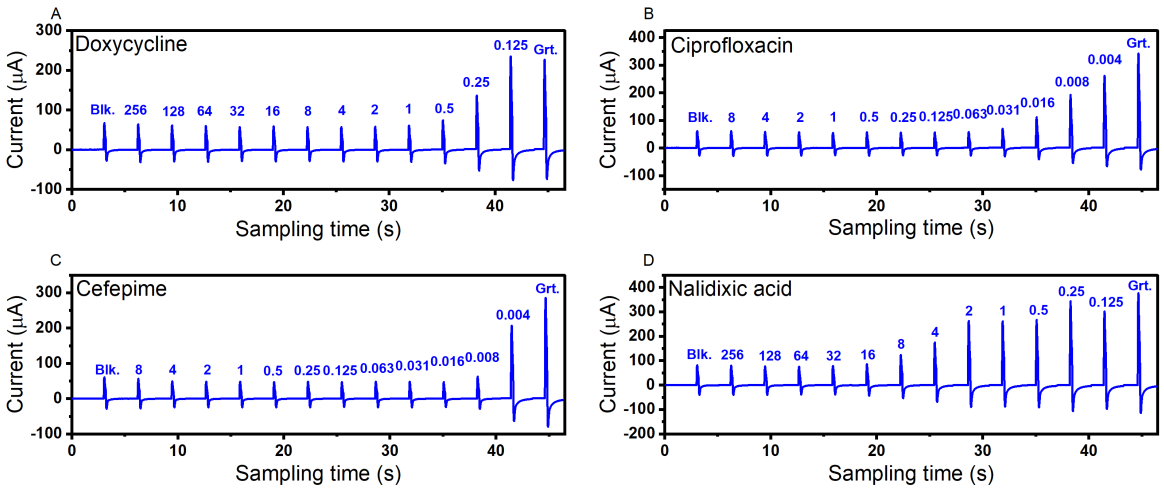

Fig. S3 Interpretable antimicrobial susceptibility profiles obtained through continuous-sampling electrochemical measurement. The profiles represent collective measurements of E. coli samples, initially incubated with doxycycline (A), ciprofloxacin (B), cefepime (C) and nalidixic acid (D) followed by exposure to ferricyanide as an electron-transport probe. The number above the peak corresponds to different antibiotic concentrations in μg/ml or control types; Blk. = blank control, Grt. = growth control.

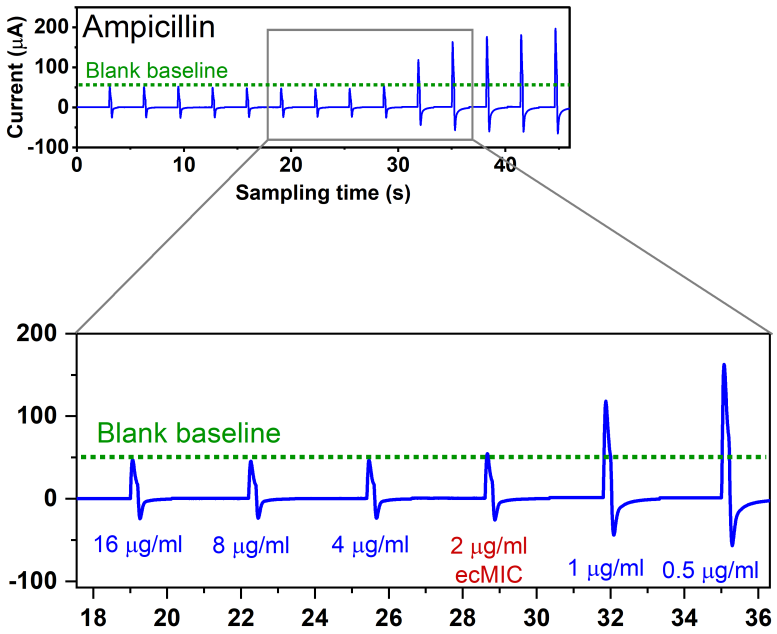

Fig. S4 Characteristics of the electrochemical susceptibility profile and determination of electrochemical minimum inhibitory concentration (ecMIC) using ampicillin as an example. To determine the ecMIC, the blank baseline is horizontally positioned along the profile based on the value of the blank's response, and the ecMIC is identified as the lowest concentration before a significant increase above the blank baseline. As a result of the interpretation, the ecMIC for ampicillin is 2 μg/ml as shown in the close-up.

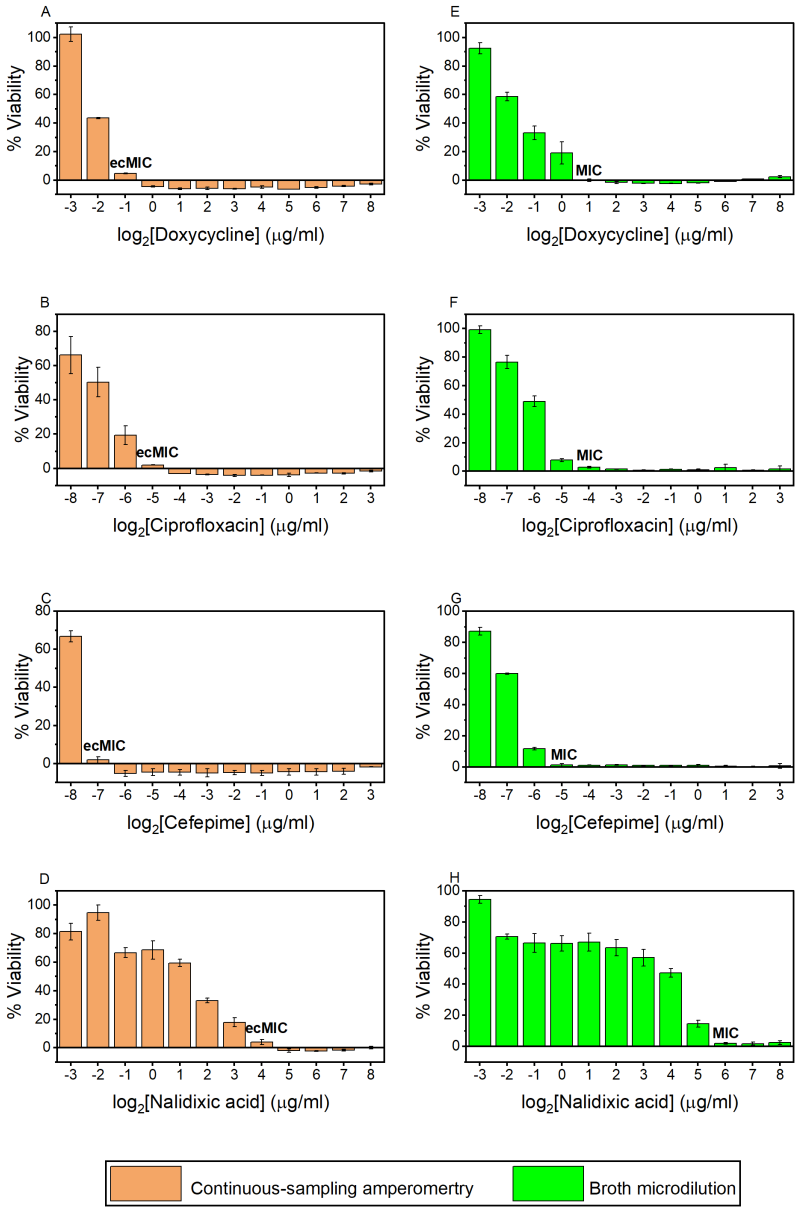

Fig. S5 Calculated bacterial viability percentages (% Viability) derived from the electrochemical susceptibility profiling (orange) with doxycycline (A), ciprofloxacin (B), cefepime (C) and nalidixic acid (D), with the determination of the electrochemical minimum inhibitory concentrations (ecMICs). The resulting viability characteristics and ecMICs are validated with the result of the microdilution method (green) for the corresponding antibiotics (E-H) with the determination of conventional minimum inhibitory concentration (MIC).

Table S1 Electrochemical minimum inhibitory concentrations (ecMICs) determined from the electrochemical readouts as susceptibility profiles.

Antibiotic	ecMIC (μg/ml)
Kanamycin	4
Ampicillin	2
Doxycycline	0.5
Imipenem	4
Ciprofloxacin	0.031
Cefepime	0.008
Nalidixic acid	16

Table S2 Comparison of the determined ecMICs and MICs with the interpreted classification of susceptibility.

Antibiotic	Electrochemical method		Microdilution method	
	ecMIC (μg/ml)	Classification*	MIC (μg/ml)	Classification*
Kanamycin	4	Susceptible	4	Susceptible
Ampicillin	2	Susceptible	2	Susceptible
Doxycycline	0.5	Susceptible	2	Susceptible
Imipenem	4	Resistant	4	Resistant
Ciprofloxacin	0.031	Susceptible	0.063	Susceptible
Cefepime	0.008	Susceptible	0.031	Susceptible
Nalidixic acid	16	Susceptible	64	Resistant

* Classifications are followed the interpretive breakpoint criteria by CLSI M100 document[6]

Table S3 Selected works of redox mediator-based electrochemical AST with their major parameters, compared to this work.

Redox mediator	Sensing platform	Electroanalysis technique	Model bacteria	Antibiotic	Antibiotic incubation period	Accuracy of determined MICs compare to standard methods	Ref.
Ferricyanide	Beaker-type; WE: Rotating Pt disk	Amperometry (30 min), Coulombmetry (2 min)	*E. coli,* *C. sporogenes*	Penicillin G, D-cycloserine, Vancomycin, Bacitracin, Cephalosporin C, Tetracycline, Erythromycin, Chloramphenicol, Streptomycin, Nalidixic acid, Rifampicin, Trimethoprim, Nystatin	10-20 min	-	[7]
Ferricyanide and dichlorophenol-indophenol	Screen-printed graphite electrode-microwell array	Cyclic voltammetry, Coulombmetry (2 min)	*E. coli*	Bacitracin, D-cycloserine, Erythromycin, Geneticin, Hygromycin, Kanamycin, Neomycin, Paromomycin, Rifampicin, Streptomycin, Trimethoprim, Vancomycin, Chloramphenicol, Nystatin, Carbenicillin, Cefotaxime, Nalidixic acid	10 min	-	[8]
Ferricyanide	Beaker-type; WE: Pt disk	Amperometry (10 min)	*E. coli,* *B. pseudomallei*	Cefepime, Ceftazidime, Ciprofloxacin, Co-Trimoxazole, Dicloxacillin, Gentamicin	15-180 min	-	[1]
Resazurin	Patterned-Au electrode nanoliter-well array	Differential pulse voltammetry	*E. coli,* *K. pneumoniae*	Ampicillin, Ciprofloxacin	1 h	nonequivalent	[9]

Table S3 *Continued*

Redox mediator	Sensing platform	Electroanalysis technique	Model bacteria	Antibiotic	Antibiotic incubation period	Accuracy of determined MICs compare to standard methods	Ref.
Tetrazolium salt derivatives and resazurin	Bacteria-immunoaffinity/paramagnetic bead with inkjet-printed electrode microchip array	Differential pulse voltammetry	*E. coli,* *B. subtilis*	Ampicillin, Cefpodoxime, Ceftriaxone, Gentamicin, Ciprofloxacin, Imipenem, Tetracycline, Nitrofurantoin, Fosfomycin	90-180 min	6 of 9 are equivalent; the rest are comparable	[10]
Resazurin	Beaker-type; WE: Sputtered Pt thin film	Differential pulse voltammetry	*E. coli,* *K. pneumoniae*	Ampicillin, Kanamycin, Tetracycline	1-4 h	-	[11]
Resazurin	Au nanoparticles /multi-walled carbon nanotubes/ screen-printed carbon	Differential pulse voltammetry	*S. gallinarum* (3 tested strains)	Ofloxacin, Penicillin	4 h	1 of 3 are equivalent; the rest are comparable	[12]
Mediatorless-exoelectrogenic process	Paper-based biobatery sensing array	Accumulative electrical energy (900 s)	*P. aeruginosa*	Gentamicin	220 min	Equivalent	[13]
Ferricyanide	Beaker-type; WE: Lysine/CeO nanoparticles / ITO	Cyclic voltammetry	*E. coli, B. subtilis*	Amoxicillin, Cefixime, Ciprofloxacin	15 min	-	[14]
Resazurin	Beaker-type; WE: Nafion/ Organic redox-active crystal/ Pyrolytic graphite sheet	Cyclic voltammetry for pH changing detection	*E. coli*	Ampicillin, Kanamycin	1 h	Equivalent	[15]
Resazurin	Resazurin/ Screen-printed electrode	Differential pulse voltammetry	*E. coli*	Gentamicin	20 min – 4 h	-	[16]

Table S3 *Continued*

Redox mediator	Sensing platform	Electroanalysis technique	Model bacteria	Antibiotic	Antibiotic incubation period	Accuracy of determined MICs compare to standard methods	Ref.
Methylene blue	Beaker-type WE: Graphene ink-modified glassy carbon	Cyclic voltammetry	*E. coli*	Ciprofloxacin, Gentamycin, Ampicillin	1 h	-	[17]
Phenazine methosulfate	Bioreactor-type; WE: Glassy carbon	Amperometry	*A. baumannii, S. aureus, E. coli, K. pneumoniae*	Tobramycin, Imipenem, Oxacillin, Ciprofloxacin	Up to 90 min	-	[18]
Ferricyanide	Two-electrode Pt mini-cell; WE: Pt disk	Pulse amperometry	*E. coli*	Kanamycin, Doxycycline, Ampicillin, Imipenem, Cefepime, Ciprofloxacin, Cefepime, Nalidixic acid	3 h	3 of 7 are equivalent; the rest are comparable	This work

References

1. K. Chotinantakul, W. Suginta and A. Schulte, *Anal. Chem.*, 2014, **86**, 10315-10322.
2. CLSI, *Methods for Dilution Antimicrobial Susceptibility Tests for Bacteria That Grow Aerobically; Approved Standard—Ninth Edition*, Clinical and Laboratory Standards Institute, 950 West Valley Road, Suite 2500, Wayne, Pennsylvania 19087, USA, 9 edn., 2012.
3. N. Elgrishi, K. J. Rountree, B. D. McCarthy, E. S. Rountree, T. T. Eisenhart and J. L. Dempsey, *J. Chem. Educ.*, 2018, **95**, 197-206.
4. D. Kim and S. Yoo, *Chemosensors*, 2022, **10**, 53.
5. S. Hannah, R. Domingo-Roca, P. A. Hoskisson, M. E. Murphy and D. K. Corrigan, *Curr. Opin. Electrochem.*, 2022, **35**, 101033.
6. CLSI, *Performance Standards for Antimicrobial Susceptibility Testing; Twenty-Second Information Supplement*, Clinical and Laboratory Standards Institute, 950 West Valley Road, Suite 2500, Wayne, Pennsylvania 19087 USA, 2012.
7. P. Ertl, E. Robello, F. Battaglini and S. R. Mikkelsen, *Anal. Chem.*, 2000, **72**, 4957-4964.
8. T. S. Mann and S. R. Mikkelsen, *Anal. Chem.*, 2008, **80**, 843-848.
9. J. D. Besant, E. H. Sargent and S. O. Kelley, *Lab Chip*, 2015, **15**, 2799-2807.
10. Y. Zhu, M. Jović, A. Lesch, L. Tissières Lovey, M. Prudent, H. Pick and H. H. Girault, *Angew. Chem. Int. Ed.*, 2018, **57**, 14942-14946.
11. P. Mishra, D. Singh, K. P. Mishra, G. Kaur, N. Dhull, M. Tomar, V. Gupta, B. Kumar and L. Ganju, *J. Microbiol. Methods*, 2019, **162**, 69-76.
12. Y. Ren, J. Ji, J. Sun, F. Pi, Y. Zhang and X. Sun, *J. Solid State Electrochem.*, 2020, **24**, 1539-1549.
13. Y. Gao, J. Ryu, L. Liu and S. Choi, *Biosens. Bioelectron.*, 2020, **168**, 112518.
14. P. Rao R, S. Sharma, T. Mehrotra, R. Das, R. Kumar, R. Singh, I. Roy and T. Basu, *Anal. Chem.*, 2020, **92**, 4266-4274.
15. A. Bolotsky, R. Muralidharan, D. Butler, K. Root, W. Murray, Z. Liu and A. Ebrahimi, *Biosens. Bioelectron.*, 2021, **172**, 112615.
16. B. Crane, J. P. Hughes, S. J. Rowley Neale, M. Rashid, P. E. Linton, C. E. Banks and K. J. Shaw, *Analyst*, 2021, **146**, 5574-5583.
17. R. Duan, X. Fang and D. Wang, *Front. Chem.*, 2021, **9**, 689735.
18. G. Tibbits, A. Mohamed, D. R. Call and H. Beyenal, *Biosens. Bioelectron.*, 2022, **197**, 113754.